Available online at www.sciencedirect.com
SCIENCE DIRECT
Journal of Organometallic Chemistry 691 (2006) 1834–1844
Journal of Organometallic Chemistry
www.elsevier.com/locate/jorganchem

Synthesis, spectroscopic and electrochemical studies of a series of transition metal complexes with amino- or bis(bromomethyl)-substituted dppz-ligands: Building blocks for fullerene-based donor–bridge–acceptor dyads

Andreas Kleineweischede, Jochen Mattay *

Organische Chemie I, Fakultät für Chemie, Universität Bielefeld, Postfach 10 01 31, 33501 Bielefeld, Germany

Received 22 September 2005; accepted 1 December 2005
Available online 14 February 2006

Abstract

Transition metal complexes with ligands based on dipyrido[3,2-*a*:2′,3′-*c*]phenazine (dppz) have been synthesized. As metal fragments the $[Ru(bpy)_2]^+$, $Re(CO)_3Cl$ and the $[Cu(PPh_3)_2]^+$ moieties have been used. The complexes containing amino- or bis(bromomethyl) substituted dppz ligands can be used for fullerene-based donor–bridge–acceptor dyads. The electronic absorption spectra of these complexes and of the dppz ligands were investigated. The dppz ligands show strong absorptions in the 300 and 390 nm region. An additional absorption band in the visible region (~440 nm) is observed for the amino-substituted dppz-ligands. Ruthenium complexes exhibited broad absorption bands at 350–500 nm arising from intraligand-based transitions and the MLCT transition. MLCT transitions of the Re(I) and Cu(I) complexes are observed as shoulders of the stronger ligand-based absorption band tailing out to 400–500 nm. The electrochemically active complexes and ligands were studied by cyclic voltammetry and square-wave voltammetry. All ligands show one first reversible one-electron reduction located at the phenazine portion. These reductions are shifted to more positive redox potentials upon complexation. Oxidation potentials for reversible processes could be determined for the Ru^{2+}/Ru^{3+} couple. For rhenium(I) and copper(I) complexes one irreversible oxidation process is observed.

Keywords: N ligands; Polypyridyl complexes; Cyclic voltammetry; UV/Vis spectroscopy

1. Introduction

Metal complexes with ligands based on dipyrido[3,2-*a*:2′,3′-*c*]phenazine (dppz) are of interest because of their interactions with DNA [1], their molecular switching properties [2] and their potential in solar energy conversion schemes [3]. In most solar energy conversion schemes based on transition metal complexes solar energy is captured through a charge-separation scheme, such as excitation to the metal-to-ligand charge-transfer (MLCT) state [4]. The advantage of using dppz-based systems is that the overlap between the metal d_π and ligand π^* orbitals is small [5], thus reducing the back electron-transfer rate. The long-lived MLCT excited states of transition metal complexes such as tris(bpy)-ruthenium(II) [6] (bpy = 2,2′-bipyridine), bis(1,10-phenanthroline)copper(I) [7] or (2,2′-bpy)rhenium(I) [8] have been widely exploited to design multicomponent molecular architectures featuring photoinduced electron- and energy-transfer processes [7,9]. Interestingly, the MLCT excited states of these compounds have a marked reducing character that, in principle, make them ideal partners for the construction of donor–acceptor systems with C_{60} fullerenes. The ability of fullerenes to act as electron acceptors make them attractive for participation in such supramolecular assemblies suitable for mimicking the natural photosynthesis process. However, not

* Corresponding author.
E-mail address: mattay@uni-bielefeld.de (J. Mattay).

0022-328X/$ - see front matter © 2005 Elsevier B.V. All rights reserved.
doi:10.1016/j.jorganchem.2005.12.008

many examples of such arrays have been reported to date. In most cases ruthenium is incorporated in these fullerene-based donor–bridge–acceptor systems [10] and only a few examples are known in which a copper [11] or rhenium [12] metal center acts as a donor.

Synthesis of fullerene-based donor–bridge–acceptor dyads in which metal fragments are incorporated can be obtained either by complexation of fullerene derivatives containing a suitable coordination site (so-called fullerene ligands) or by reaction of C_{60} or fullerene derivatives with transition metal complexes bearing functionalities appropriate for the attachment of these complexes to the fullerene core. Recently, we reported on the synthesis of amino- and bis(bromomethyl)-substituted dppz derivatives as building blocks for pyrazino-functionalized fullerene dyads containing the bpy fragment [13]. For the preparation of molecular architectures that combine the fullerene as acceptor and a metal fragment as donor, we follow the synthetic strategies – condensation of diamines with fullerene substituted cyclohexane-1,2-dione or Diels–Alder reaction of C_{60} with *o*-quinodimethanes generated in situ from the corresponding bis(bromomethyl) derivative – leading to these pyrazino-functionalized fullerene dyads as depicted in Scheme 1. Therefore, synthesis of transition metal complexes with amino- and bis(bromomethyl)-substituted dppz ligands is required.

Herein, we report on the preparation of dppz complexes containing the $[Ru(bpy)_2]^{+}$, the $Re(CO)_3Cl$ and the $[Cu(PPh_3)_2]^{+}$ fragment that are potential building blocks for fullerene-based donor–bridge–acceptor dyads. The exceptional features of using copper(I) and rhenium(I) complexes are as follows. (i) The $Re(CO)_3Cl$ and $[Cu(PPh_3)_2]^{+}$ moiety do not possess chromophores in the visible region, thus the spectroscopy of the complexes is more readily interpreted. (ii) Copper(I) and rhenium(I) complexes offer interesting contrasts in photophysical behaviour. The excited-state properties of copper(I) complexes are strongly affected by the substituents on the ligands used [14]. For rhenium complexes the photophysical properties, such as excited state lifetime, depend more on the energy gap law than on steric effects [15]. (iii) The metal fragments have different π-acid properties perturbing the ligand to different extents when complexed.

2. Results and discussion

2.1. Synthesis of transition metal complexes with dppz ligands

In general, all the complexes described herein were prepared by complexation of the dppz ligands with suitable metal precursors such as *cis*-$Ru(bpy)_2Cl_2$, $Re(CO)_5Cl$ and $[Cu(CH_3CN)_2(PPh_3)_2](BF_4)$ as depicted in Scheme 2. 11-Nitrodipyrido[3,2-*a*:2′,3′-*c*]phenazine (ndppz), 11-aminodipyrido-[3,2-*a*:2′,3′-*c*]phenazine (adppz), 11,12-dinitrodipyrido[3,2-*a*:2′,3′-*c*]phenazine (dndppz), 11,12-diaminodipyrido[3,2-*a*:2′,3′-*c*]phenazine (dadppz) and 11,12-bis(bromomethyl)dipyrido[3,2-*a*:2′,3′-*c*]phenazine (dbrdppz) were used as ligands. The preparation of the above-mentioned ligands was described elsewhere [13]. Synthesis of the ligands ndppz and dndppz was based on Schiff-base condensation of 1,10-phenanthroline-5,6-dione with the nitro-substituted *o*-phenylen-derivatives. Reduction of ligands ndppz and dndppz led to the formation of ligands adppz and dadppz. Preparation of the bis(bromomethyl)-substituted dppz derivative was performed by bromination of 11,12-dimethyldipyrido[3,2-*a*:2′,3′-*c*]phenazine.

Synthesis of $[Ru(bpy)_2(dppz)]^{2+}$ complexes was easily carried out by reaction of one equivalent *cis*-$Ru(bpy)_2Cl_2$ [16] and 1.2 equivalents of the dppz ligands in ethanol/water according to a literature procedure [17]. With the exception of complex $[Ru(bpy)(adppz)]^{2+}$ [18] all compounds are new complexes. All complexes have been characterized by ^1H NMR except the complex $[Ru(bpy)_2(dbrdppz)]^{2+}$ that is

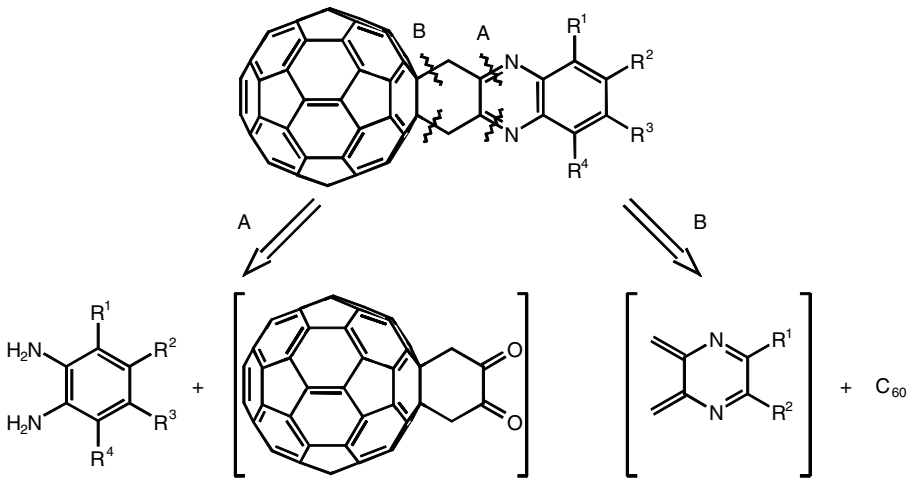

Scheme 1. Synthesis of pyrazino-functionalized fullerene dyads by condensation of fullero-cyclohexane-1,2-dione with aromatic diamines (path A) or by Diels–Alder addition of *o*-quinodimethanes (path B).

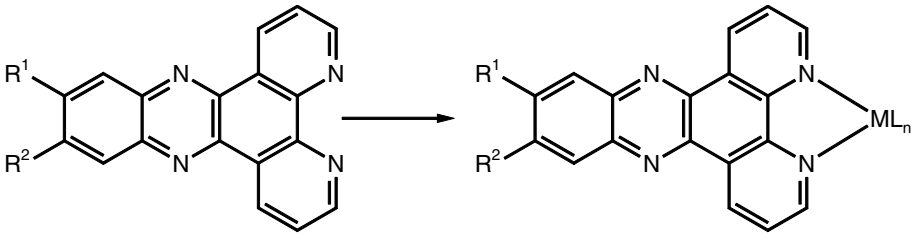

ndppz: $R^1 = H$, $R^2 = NO_2$
dndppz: $R^1 = R^2 = NO_2$
adppz: $R^1 = H$, $R^2 = NH_2$
dadppz: $R^1 = R^2 = NH_2$
dbrdppz: $R^1 = R^2 = CH_2Br$

1a-e: $[Ru(bpy)_2]^{2+}$
2a-e: $[Re(CO)_3Cl]$
3a-e: $[Cu(PPh_3)_2]^{+}$

a: L = ndppz
b: L = dndppz
c: L = adppz
d: L = dadppz
e: L = dbrdppz

Scheme 2. Synthesis of complexes **1a–e**, **2a–e** and **3a–e** by complexation of the $[Ru(bpy)_2]^{2+}$, $[Re(CO)_3Cl]$ and $[Cu(PPh_3)_2]^{+}$ metal fragment to the dppz ligands.

insoluble in all common organic solvents. Due to the poor solubility of the amino-functionalized ruthenium complexes the NMR spectra of these complexes are not well resolved. Therefore, the spectra will be discussed for the nitro-substituted complexes. It is convenient to consider the dppz as a combination of phenanthroline (phen) and phenazine (phz) as the molecular orbitals present in dppz adopt those characteristics [19]. Upon complexation these fragments were influenced to a different extent. The protons in *meta* and *para* position to the nitrogen in the phen fragment of the dppz ligands remain nearly unaffected. In contrast, complexation of the dppz ligands the protons in *ortho* position were shifted up-field relative to the free ligand. This is due to the electron density reduction at the nitrogens upon complexation with the $Ru(bpy)^{2+}$ fragment. No significant effect on the chemical shifts for the phenazine protons was observed. Furthermore, eight signals for the bpy ligands of the $[Ru(bpy)_2]^{2+}$ fragment can be detected consisting of two sets of four chemical inequivalent pyridine hydrogens showing the same spectral pattern and identical coupling constants. This effect can be explained by different orientations of the pyridyl rings of the bpy ligands relative to the dppz ligand resulting in two sets of pyridine protons as shown by the calculated structure of the $[Ru(bpy)_2(dndppz)]^{2+}$ complex (Fig. 1).

In the mass spectra signals for the $[M - 2PF_6^-]^{2+}$ ions for all complexes are observed. Signals due to a successive fragmentation of the hexafluorophosphate counterion or hydrolysis of the hexafluorophosphate ion are not observed in the mass spectra. Furthermore, the observed spectral pattern is in good agreement with the calculated mass distribution for $[M - 2PF_6^-]^{2+}$ ions.

Preparation of the complexes $[Re(CO)_3(ndppz)Cl]$ **2a** and $[Re(CO)_3(adppz)Cl]$ **2b** has already been published by Loeb et al. [20]. Rhenium complexes **2c–e** containing the ligands dndppz, dadppz an dbrdppz were prepared according to this literature procedure. In a typical experiment a solution of equimolar amounts of $Re(CO)_5Cl$ and

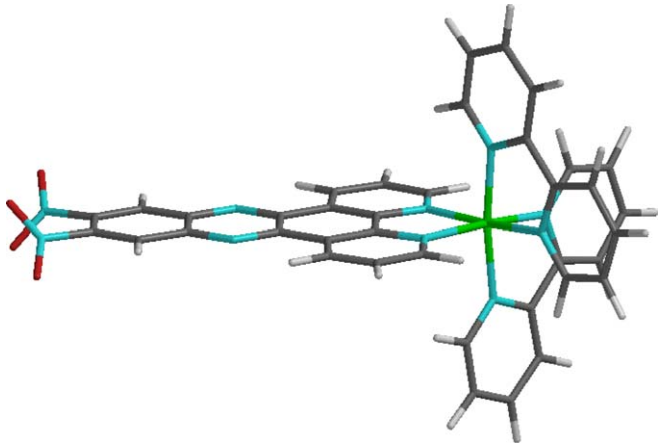

Fig. 1. Calculated structure of the $[Ru(bpy)_2(dndppz)]^{2+}$ complex **1b** (semiempirical PM3, Titan).

the appropriate ligand in degassed toluene was refluxed for 24 h under argon atmosphere. The NMR data support the idea of the ligands acting as phen and phenazine ring systems with the metal perturbing the phen and the substituents the phenazine portion. When the substituted dppz ligands are coordinated to Re in the $[Re(CO)_3(L)Cl]$ complexes (L = dppz ligand) the phen fragment protons are dominated by the effect of coordination. These protons show a significant down-field shift reflecting the change in nitrogen atom hybridization because of coordination with the subsequent deshielding effect on the protons [21]. The phenazine protons are also displaced to lower field, but the effect of the dppz substituents is retained. This is in good agreement with the results obtained by Loeb et al. [20]. ESI as well as MALDI-Tof mass spectra of the complexes were not available because the complexes decompose under the conditions of the experiment. A good diagnostic criterium for the formation of the rhenium complexes is the presence of sharp absorption bands for the CO ligands between 1900 and 2050 cm^{-1} in the IR spectrum

typical for a facial orientation of the CO ligands (see Table 1) [22]. According to Stufkens et al. [23] the absorption bands at $>2000\,cm^{-1}$ can be ascribed to the carbonyl ligands in *cis*-position to the dppz ligand. Observation of two partly resolved absorption bands at lower energy is due to a distorted C_{3v} symmetry at the metal center. These bands are assigned to the CO ligands in *trans*-position to the dppz ligand.

Copper complexes **3a**–**e** were obtained by stirring one equivalent of $[Cu(CH_3CN)_2(PPh_3)_2](BF_4)$ and one equivalent of the dppz ligand [24]. The precursor complex $[Cu(CH_3CN)_2(PPh_3)_2](BF_4)$ was prepared by the reaction of $[Cu(CH_3CN)_4](BF_4)$ with two equivalents of PPh_3 in acetonitrile solution [25]. Yields for the Cu dppz complexes range from 67% to 91%, respectively. The ^1H NMR spectra of these complexes are dominated by the signals of the phenyl protons of the PPh_3 ligands at $\delta = 7.16$–7.22 ppm. The copper complexes also show smaller shifts at the phenazine relative to the phenanthroline fragment. The effect is less than for the rhenium(I) complexes consistent with the less perturbative effect of the $[Cu(PPh_3)_2]^+$ moiety. Formation of the mononuclear Cu(I) dppz complexes was assured by detection of the signals of the $[M - BF_4]^+$ ion in the ESI mass spectra of the complexes. In addition, signals at $m/z = 587$ can be observed which can be assigned to $[Cu(PPh_3)_2]^+$ indicating dissociation of the complexes. This can be confirmed by detection of signals arising from the dppz ligand.

An alternative route to the amino-functionalized dppz complexes is the palladium-catalyzed hydrogen reduction of the nitro substituents of the dppz ligands (Scheme 3). This route is not appropriate for the rhenium complexes due to possible reduction of the CO ligands leading to decomposition of the complexes. Therefore, only the synthesis of the amino-functionalized Ru(II) **1c**, **1d** and Cu(I) complexes **3c**, **3d** were performed by this method. The nitro-substituted complexes were quantitatively transformed into the corresponding amino-functionalized complexes $[Ru(bpy)_2L](PF_6)$ and $[Cu(CH_3CN)_2L](BF_4)$ (L = adppz, dadppz).

Table 1
Infrared spectral data for $[Re(CO)_3(dppz)Cl]$ complexes in the carbonyl region

$[Re(CO)_3(L)Cl]$	dppz ligand	$\tilde{\nu}_{CO}/cm^{-1}$
2a	ndppz	2031, 1905
2b	dndppz	2028, 1918, 1891
2c	adppz	2021, 1914, 1901
2d	dadppz	2024, 1901
2e	dbrdppz	2021, 1913, 1897

2.2. UV/Vis absorption spectra

The electronic absorption spectra of the ligands are presented in Table 2. The absorption spectra of these ligands show $\pi^* \leftarrow \pi$ transitions in the 390 nm region. Stronger ligand-centered transitions are observed at wavelengths shorter than 300 nm. The band position seem to be rather insensitive to substitution of the phenazine fragment. This indicates that the substituents affects the energy of both orbitals involved in the transition to a similar extent. In contrast, the lowest energy absorption band of the amino-substituted dppz derivatives appear at much lower energy (~440 nm). As an example the UV/Vis spectrum of the dadppz ligand is shown in Fig. 2. There has been a report that the lowest energy absorption of phenazine also experiences a considerable bathochromic shift upon 2-amino substitution [26]. The influence of the amino groups on the electronic spectra results from the conjugation of the nitrogen free electron pair with the phenazine π-system, thus, increasing the electron density on the phenazine portion of the dppz ligand.

Table 2
Electronic absorption data for dppz ligands in dichloromethane

dppz ligand	λ_{max}/nm ($\varepsilon/10^4\,M\,cm^{-1}$)
ndppz	246 (4.64), 254 (4.23), 287 (4.54), 295 (4.76), 303 (4.05), 368 (1.79), 386 (1.49)
dndppz	228 (5.45), 233 (5.25), 249 (4.40), 293 (2.01), 304 (1.67), 389 (0.61)
adppz	238 (7.48), 251 (6.57), 293 (6.94), 308 (7.02), 447 (2.61)
dadppz	229 (5.81), 262 (3.97), 276 (4.26), 291 (4.52), 308 (4.90), 396 (1.55), 442 (2.62)
dbrdppz	247 (4.48), 253 (4.16), 287 (4.37), 293 (4.55), 303 (3.98), 378 (1.27), 390 (1.91)

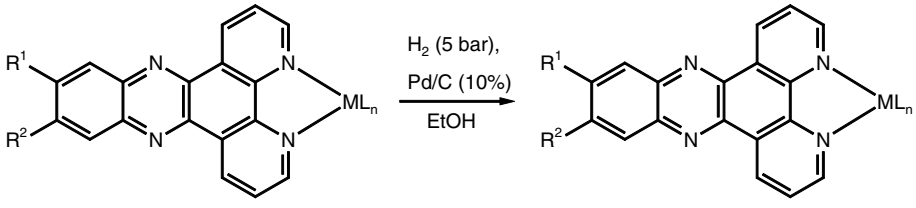

1a, **3a** ($R^1 = H$, $R^2 = NO_2$)
1b, **3b** ($R^1 = R^2 = NO_2$)
1c, **3c** ($R^1 = H$, $R^2 = NH_2$)
1d, **3d** ($R^1 = R^2 = NH_2$)

Scheme 3. Synthesis of the amino-substituted Ru(II) complexes **1c**,**d** and Cu(I) complexes **3c**,**d** by reduction of the corresponding nitro-substituted complexes.

Due to the planar and extended π-system of the dppz derivatives these compounds may form dimeric species or higher aggregates by π–π-stacking. Formation of such aggregates can be monitored by measuring concentration-dependent absorption spectra for the dppz ligands because solute–solute interactions will result in changes of the spectral pattern. The ligands dndppz and dadppz were investigated, but no changes in the spectral pattern were observed indicating that solute–solute interactions are absent. In Fig. 3, the absorption spectra for dadppz measured at different concentrations are shown.

The electronic absorption spectra of the Ru(II) dppz complexes were measured in acetonitrile at 25 °C and the data collected are presented in Table 3. In the absorption spectra of the $[Ru(bpy)(dppz)]^{2+}$ complexes **1a–e** the high-intensity absorption band at about 300 nm can be ascribed to the ligand-centered $\pi^* \leftarrow \pi$ transition [18]. A broad band at lower energy at about 350–500 nm consists of both the ligand-centered $\pi^* \leftarrow \pi/\pi^* \leftarrow$ n transitions of the dppz ligands and the spin-allowed metal-to-ligand charge-transfer (^{1}MLCT) band from the Ru(II) center to the diimine ligands [27]. The dppz ligand is a prototypical acceptor with different redox and optical acceptor π^* orbitals [19,28]. The lowest unoccupied π MO in Ru(II) dppz complexes is localized at the phenazine portion of the dppz ligand and of b_1(phz) type. This seemed to have little contribution and effects from the α-diimine chelate site and the metal coordinated there. Thus, MLCT transitions to that b_1(phz) MO are very weak and usually not observable. The MLCT transitions observed originate from overlap between d_π orbitals of the coordinated ruthenium metal center and higher lying α-diimine-based unoccupied MOs of the $b_1(\psi)$ and $a_2(\chi)$ type [28c] (see Fig. 4).

The absorption spectra of the rhenium(I) and copper(I) complexes are easier to interpret as the $[Re(CO)_3Cl]$ and the $[Cu(PPh_3)_2]^+$ moieties do not have any further chromophores. The electronic spectra of Re(I) and Cu(I) complexes are dominated by the dppz bands described above. Nevertheless, the coordination to the metal center is evidenced by MLCT transitions in the visible region tail-

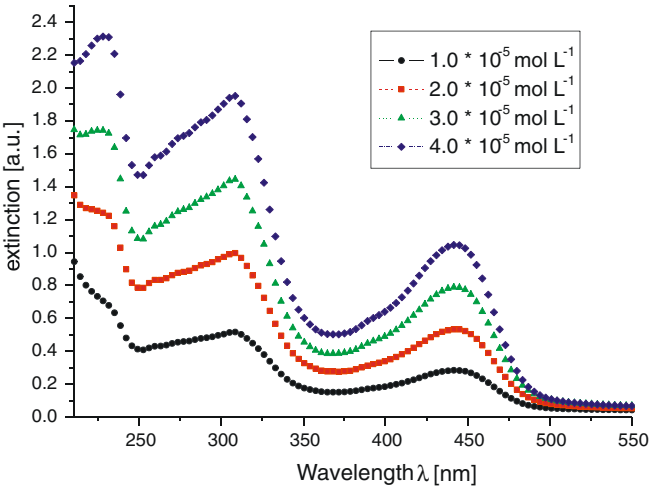

Fig. 3. Concentration-dependent absorption spectra of dadppz.

Table 3
Electronic absorption data for $[Ru(bpy)_2(dppz)]^{2+}$ complexes **1a–e** in acetonitrile

$[Ru(bpy)_2L]^{2+}$	Ligand	λ_{max}/nm ($\varepsilon/10^4$ M cm^{-1})
1a	ndppz	247 (3.83), 287 (7.95), 358 (1.59), 442 (1.44)
1b	dndppz	245 (3.81), 252 (sh), 288 (7.87), 356 (1.55), 374 (), 441 (1.46)
1c	adppz	256 (4.62), 286 (7.35), 316 (4.51), 469 (2.53)
1d	dadppz	255 (4.55), 288 (7.27), 318 (4.47), 468 (2.49)
1e	dbrdppz	248 (3.78), 285 (7.91), 353 (1.57), 441 (1.43)

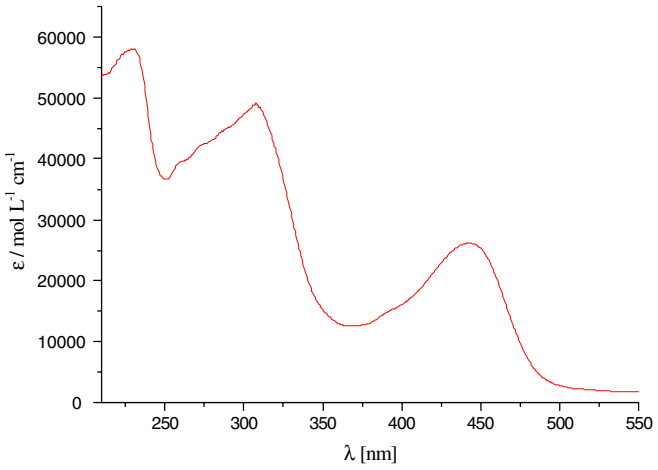

Fig. 2. UV/Vis absorption spectrum of the ligand dadppz in dichloromethane.

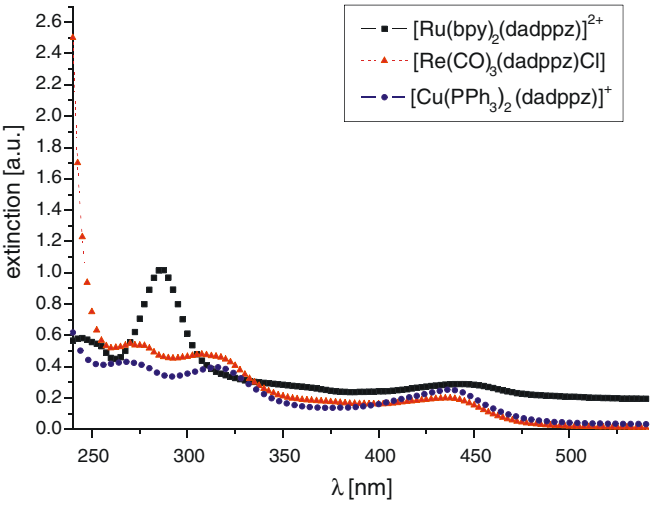

Fig. 4. UV/Vis absorption spectra of the diamino-substituted complexes **1d**, **2d**, and **3d**.

ing out to 400–500 nm that appear as a shoulder of the more intense $\pi^* \leftarrow \pi$ ligand bands. Extension of these shoulders into the red is observed for complexes that are easier to reduce. The lower intensity and higher energy of MLCT bands of complexes (α-diimine)ML_n with M = Cu(I) and Re(I) is well established [29–31] (see Tables 4 and 5).

2.3. Cyclic voltammetry and square wave voltammetry

Electrochemical measurements of the ligands in dichloromethane were carried out in the range between +1.0 V and −2.10 V vs. the ferrocene/ferrocinium (fc/fc^+) couple. The data collected are presented in Table 3. In the investigated region the nitro-substituted dppz derivatives show two reversible one-electron reduction processes. The distance between these reductions is nearly the same for both compounds ($\Delta E_{red} = E^2_{red} - E^1_{red} = 0.45$ V for ndppz; 0.48 V for dndppz). Introduction of a second electron-withdrawing NO_2 substituent leads to a more positive redox potential for the dinitro derivative than for the mono-substituted ligand ndppz. Thus, the former compound is easier to reduce. This observation is in good agreement with the electron-withdrawing properties of the NO_2 substituent as such substituents decreases the electron density of the dppz ligand. In case of the amino-substituted dppz ligands only one reduction can be observed. Due to the electron-donating properties of the amino substituents the redox potential for the first reduction process is shifted to more negative potentials. Addition of a second amino group makes the ligand harder to reduce. This is in accordance with a further shift of the redox potential to more negative values. Data for the bis(bromomethyl)-substituted dppz ligand were not obtained mainly due to decomposition of this compound under the condition of the experiment. Bis(bromomethyl)-substituted aromatics can be easily transformed into the corresponding *o*-quinodimethanes by reductive elimination (see Table 6).

The electrochemically active complexes were studied using cyclic voltammetry and square wave voltammetry. The latter technique was used because of its superior resolution. The electrochemical measurement of the $[Ru(bpy)_2(dppz)]^{2+}$, $[Re(CO)_3(dppz)Cl]$ and $[Cu(PPh_3)_2(dppz)]^+$ complexes were carried out in the range between +1.4 and −2.6 V vs. the fc/fc^+ couple using acetonitrile or dichloromethane as solvent. Due to decomposition of the dbrdppz ligand no data of the corresponding complexes **1e**, **2e** and **3e** were available.

The data obtained for the ruthenium complexes **1a**–**d** are summarized in Table 7. In the positive region, the ruthenium complexes exhibited reversible one-electron redox peaks due to the oxidation of the ruthenium metal. For all complexes the oxidation assigned to the Ru^{2+}/Ru^{3+} couple was observed at +0.95 V. This oxidation process is not affected by the different electron-withdrawing or electron-donating dppz ligands. In the negative region, the cyclovoltammograms became less well-defined. The voltammogram of the amino-substituted complex **1c** showing at least eight reversible one-electron reductions is depicted in Fig. 5.

The redox properties of the ruthenium complex **1a** will be discussed in detail. To determine the exact redox potentials square wave voltammetry was used. The one-electron reductions at approximately −1.80 and −2.0 V can be unambiguously assigned to the bpy ligands as shown by comparison with the data available in the literature [18,19,28]. The reductions at more negative potentials may also originate from reductions based on the bpy ligand. The phenazine site is only slightly coupled electronically to the ruthenium ion as shown by the low potential

Table 4
Electronic absorption data for $[Re(CO)_3(dppz)Cl]$ complexes **2a**–**e** in dichloromethane

$[Re(CO)_3(L)Cl]$	Ligand	λ_{max}/nm ($\varepsilon/10^4$ M cm^{-1})
2a	ndppz	256 (5.68), 288 (5.64), 324 (1.83), 386 (sh)
2b	dndppz	254 (5.71), 287 (5.61), 323 (1.76), 388 (sh)
2c	adppz	262 (5.41), 268 (4.33), 307 (4.28), 424 (1.49)
2d	dadppz	269 (5.45), 276 (5.35), 308 (4.77), 316 (sh), 436 (1.98)
2e	dbrdppz	287 (6.47), 373 (1.08), 389 (1.43)

Table 5
Electronic absorption data for $[Cu(PPh_3)_2(dppz)]^+$ complexes **3a**–**e** in dichloromethane

$[Cu(PPh_3)_2(L)]^+$	Ligand	λ_{max}/nm ($\varepsilon/10^4$ M cm^{-1})
3a	ndppz	263 (sh), 278 (7.48), 292 (6.96), 303 (sh), 363 (2.21), 380 (2.15)
3b	dndppz	261 (6.03), 298 (3.95), 373 (1.67), 387 (1.43)
3c	adppz	261 (3.69), 297 (3.47), 441 (2.25)
3d	dadppz	267 (3.58), 315 (3.31), 437 (2.08)
3e	dbrdppz	273 (7.31), 285 (sh), 367 (1.29), 387 (1.53)

Table 6
Electrochemical data[a] for dppz ligands in dichloromethane

dppz ligand	E^1_{red}/V[b]	E^2_{red}/V[b]
ndppz	−1.50	−1.95
dndppz	−1.35	−1.83
Adppz	−1.87	–
dadppz	−2.04	–
dbrdppz	–[c]	–[c]

[a] Recorded with a platinum disk electrode with 0.1 V s^{-1} scan rate.
[b] Referenced to a silver wire, calibrated with the ferrocene/ferrocinium couple.
[c] No data available due to decomposition of the ligand.

Table 7
Electrochemical data[a] for $[Ru(bpy)_2(dppz)]^{2+}$ complexes **1a–d** in acetonitrile

$[Ru(bpy)_2(L)]^{2+}$	Ligand	E_{Ox}/V[b]	E_{red}/V[b]
1a	ndppz	+0.95	−0.83, −1.34, −1.73, −1.82, −2.04, −2.28, −2.42
1b	dndppz	+0.95	−0.79, −1.21, −1.50, −1.85, −2.05, −2.21, −2.35
1c	adppz	+0.97	−0.96, −1.15, −1.33, −1.59, −1.81, −2.02, −2.32, −2.51
1d	dadppz	+0.95	−0.98, −1.17, −1.39, −1.62, −1.84, −2.03, −2.38, −2.57

[a] Recorded with a platinum disk electrode with 0.1 V s^{-1} scan rate.
[b] Referenced to a silver wire, calibrated with the ferrocene/ferrocinium couple.

displacement (ca. +0.3 V) between the free and coordinated dppz. This displacement lies between +0.1 and +0.5 V for most of the complexes of the $[Ru(bpy)_2L]^{2+}$ family, where L is a stronger π acceptor than bpy itself [32]. As shown in Fig. 5 three additional reversible one-electron reductions are observed in the range between −0.80 and −1.75 V. The first and second reduction potential of the free ndppz ligand was observed at −1.50 and −1.95 V, respectively. Displacement of these reductions by ca. 0.3 V to more positive potentials upon coordination will result in reduction potentials at −1.20 and −1.65 V. In the spectrum two reversible one-electron transfer processes were observed at −1.34 and −1.73 V which can be attributed to the first and second reduction potential of the phenazine fragment of the dppz ligand. The reduction observed at −0.83 V may probably arise from impurities not identified to date.

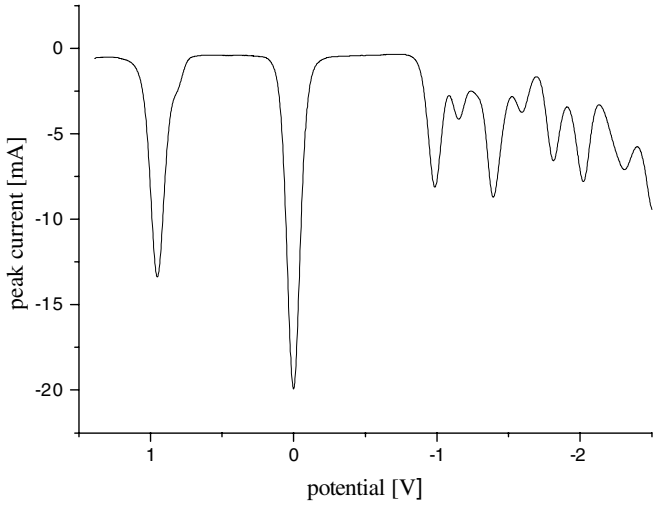

Fig. 5. Square-wave voltammogram of the $[Ru(bpy)_2(adppz)]^{2+}$ complex **1c** in acetonitrile (recorded with a platinum disk electrode with 0.1 V s^{-1} scan rate, referenced to a silver wire, calibrated with the ferrocene/ferrocinium couple).

Electrochemical data for the copper(I) and rhenium(I) complexes are presented in Tables 8 and 9. The rhenium(I) complexes are all easier to reduce than their ligand counterparts. This can be explained by a strong interaction of the $[Re(CO)_3Cl]$ fragment with the dppz ligand, stabilizing the LUMO through the π-acid characteristics of the CO ligands [32]. However, Re(I) dppz complexes with electron-withdrawing ligands are more readily reduced relative to the complexes with ligands bearing electron-donating groups. Thus, the redox behaviour of the free ligands is retained when complexed to the $[Re(CO)_3Cl]$ moiety. The differences observed between differing rhenium complexes is similar to that observed between the corresponding free phenazines. Therefore the reductions are assigned as ligand based. All rhenium complexes show an irreversible one-electron oxidation at +1.25 V which can be ascribed to the Re^{+}/Re^{2+} couple [24,33]. The potentials are not affected by substitution of the dppz ligands. The results of the complexes studied in this work are in good agreement with those obtained by Gordon et al. [24,33].

The $[Cu(PPh_3)_2]^{+}$ fragment has a much weaker effect on the energies of the ligand. Thus, binding of the ligands to copper(I) has almost no effect on the redox potentials. This is evidenced by the small stabilization in reduction potentials on going from free ligand to copper(I) complex [34]. The redox potentials of the dppz ligands are shifted only by ~0.02 V to more positive potentials. Like the rhenium complexes, irreversible one-electron oxidations corresponding to oxidation of the Cu(I) metal center to Cu(II) are observed at ~0.95 V. Again, the oxidation potentials showed no significant effect arising from the different substitution of the dppz ligands. The values for the oxidation

Table 8
Electrochemical data[a] for $[Re(CO)_3(dppz)Cl]$ complexes **2a–d** in dichloromethane

$[Re(CO)_3(L)Cl]$	Ligand	E_{Ox}/V[b,c]	E_{red}/V[b]
2a	ndppz	+1.24	−1.28, −1.88
2b	dndppz	+1.26	−1.19, −1.67
2c	adppz	+1.26	−1.63
2d	dadppz	+1.25	−1.86

[a] Recorded with a platinum disk electrode with 0.1 V s^{-1} scan rate.
[b] Referenced to a silver wire, calibrated with the ferrocene/ferrocinium couple.
[c] All oxidations are irreversible.

Table 9
Electrochemical data[a] for $[Cu(PPh_3)_2(dppz)]^{+}$ complexes **3a–d** in dichloromethane

$[Cu(PPh_3)_2(L)]^{+}$	Ligand	E_{Ox}/V[b,c]	E_{red}/V[b]
3a	ndppz	+0.93	−1.48, −1.92
3b	dndppz	+0.94	−1.34, −1.81
3c	adppz	+0.93	−1.85
3d	dadppz	+0.96	−2.02

[a] Recorded with a platinum disk electrode with 0.1 V s^{-1} scan rate.
[b] Referenced to a silver wire, calibrated with the ferrocene/ferrocinium couple.
[c] All oxidations are irreversible.

potentials for the Cu^{+}/Cu^{2+} redox pair differ from that reported by Gordon et al. [33]. The oxidation potentials reported herein are shifted to more positive redox potential by ca. 0.3 V. To date there is no explanation for the different results.

3. Conclusion

In the present work we described the synthesis of transition metal complexes of substituted dppz ligands bearing nitro, amino or bromomethyl substituents. Complexation of the metal precursors $Ru(bpy)_2Cl_2$, $Re(CO)_5Cl$ or $[Cu(CH_3CN)_2(PPh_3)_2](BF_4)$ to the dppz ligands gave the desired polypyridyl complexes. All the complexes show strong absorptions in the UV region (~300 nm) assigned to ligand-centered $\pi^* \leftarrow \pi$ transitions. In the visible region all complexes exhibited the ^{1}MLCT transition from the metal center to the diimine ligand. In case of the rhenium and copper complexes MLCT shoulders around 370 nm were observed which overlap with the typical strong intraligand absorption of dppz. The electrochemical properties of the complexes were also investigated. Similarity of the first reduction potentials of all complexes confirmed the phenazine-based π orbital as the lowest unoccupied MO. For the ruthenium complexes, reductive electron-transfer processes were observed at potentials lower than −1.80 V that can be ascribed to reductions on the bpy ligand of the $[Ru(bpy)_2]^{2+}$ fragment.

4. Experimental section

NMR spectra were recorded on a Bruker DRX 500 spectrometer at 293 K with solvent peaks as internal reference if not otherwise noted. IR Spectra were recorded using the IR spectrometer 841 (Perkin–Elmer, Überlingen, Germany). ESI spectra were recorded using an Esquire 3000 ion trap mass spectrometer (Bruker Daltronic GmbH, Bremen, Germany) equipped with a standard ESI source. Samples were introduced by direct infusion with a syringe pump. Nitrogen served both as the nebulizer gas and the dry gas. Nitrogen was generated by a Bruker nitrogen generator NGM 11. Helium served as cooling gas for the ion trap. UV/Vis spectra were measured on a Perkin–Elmer Lambda 40 spectrophotometer. Electrochemical measurements (cyclic voltammetry and square-wave voltammetry) were performed with the potentiostat PAR 273 A (EG&G Princeton Applied Research, USA). A conventional three-electrode configuration was used, with a platinum disk of 2.2 mm-diameter sealed in glass as working electrode. The counter electrode consisted of a platinum wire and the quasi-reference electrode was a silver wire. For the electrochemical measurements of the ligands, the copper and rhenium complexes CH_2Cl_2, freshly distilled over P_4O_{10}, was used as a solvent. In the case of the ruthenium complexes CH_3CN, freshly distilled over P_4O_{10}, was used as a solvent. The base electrolyte was 0.1 M tetra-*n*-butylammonium hexafluorophosphate. Potentials are quoted vs. the ferrocene/ferrocinium couple (0.0 V), and all potentials were referenced to internal ferrocene added at the end of the experiment.

Rheniumpentacarbonylchloride was purchased from Aldrich and used without further purification. The dppz ligands were synthesized as described elsewhere [13]. $[Ru(bpy_2)_2]Cl_2$ [16] and $[Cu(CH_3CN)_2(PPh_3)_2]BF_4$ [25] were prepared according to the literature procedures.

4.1. General procedure for the synthesis of ruthenium complexes

0.2 mmol (97 mg) *cis*-$Ru(bpy)_2Cl_2$ and 0.24 mmol of the appropriate dppz ligand were suspended in 50 ml of a degassed ethanol:water solution (1:1). The resulting suspension was then refluxed for 24 h under Argon atmosphere. After cooling the reaction mixture a saturated ammonium hexafluorophosphate solution was added until no further precipitation of the complexes was observed. The solid was filtered off and washed with diethylether and water. The crude product was dried in vacuo. In Scheme 4 numbering of the carbon atoms is shown in order to follow the assignment of the ^{1}H-NMR signals of the dppz ligands.

4.1.1. $[Ru(bpy)_2(ndppz)](PF_6)_2$ (**1a**)

75%, ^{1}H NMR (CD_3CN, 500.1 MHz): δ (ppm) = 7.26 (ddd, 2H, J = 6.9 Hz/5.7 Hz/1.3 Hz, $H^{pyridyl}$), 7.46 (ddd, 2H, J = 6.9 Hz/5.7 Hz/1.3 Hz, $H^{pyridyl}$), 7.74 (d, 2H, J = 5.7 Hz, $H^{pyridyl}$), 7.84 (d, 2H, J = 5.7 Hz, $H^{pyridyl}$), 7.91 (m, 2H, H^2 and H^7), 8.02 (t, 2H, J = 8.2 Hz, $H^{pyridyl}$), 8.11 (m, 2H, J = 8.2 Hz/6.9 Hz/1.3 Hz, $H^{pyridyl}$), 8.21 (m, 2H, H^3 and H^6), 8.52 (d, 2H, J = 8.2 Hz, $H^{pyridyl}$), 8.55 (d, 2H, J = 8.2 Hz, $H^{pyridyl}$), 8.63 (d, 1H, J = 9.4 Hz, H^{13}), 8.76 (dd, 1H, J = 9.4 Hz/2.5 Hz, H^{12}), 8.88 (d, 1H, J = 2.5 Hz, H^{10}), 9.65 (dd, 2H, J = 8.2 Hz/1.3 Hz, H^1 and H^8); MS (ESI): m/z = 370.6 ($[M - 2PF_6^-]^{2+}$; calc.: 371.4).

4.1.2. $[Ru(bpy)_2(dndppz)](PF_6)_2$ (**1b**)

81%, ^{1}H NMR (CD_3CN, 500.1 MHz): δ (ppm) = 7.26 (m, 2H, J = 6.9 Hz/5.7 Hz/1.3 Hz, $H^{pyridyl}$), 7.47 (m, 2H, J = 6.9 Hz/5.7 Hz/1.3 Hz, $H^{pyridyl}$), 7.73 (d, 2H, J = 5.7 Hz, $H^{pyridyl}$), 7.83 (d, 2H, J = 5.7 Hz, $H^{pyridyl}$), 7.93 (dd, 2H, J = 8.2 Hz/5.0 Hz, H^2 and H^7), 8.02 (m, 2H, J = 8.2 Hz/6.9 Hz/1.3 Hz, $H^{pyridyl}$), 8.11 (m, 2H, J = 8.2 Hz/6.9 Hz/1.3 Hz, $H^{pyridyl}$), 8.24 (dd, 2H,

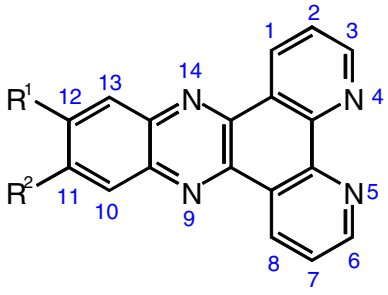

Scheme 4. Atom numbering in the dppz ligands.

$J = 5.0$ Hz/1.3 Hz, H^3 and H^6), 8.52 (d, 2H, $J = 8.2$ Hz, $H^{pyridyl}$), 8.55 (d, 2H, $J = 8.2$ Hz, $H^{pyridyl}$), 9.12 (s, 2H, H^{10} and H^{13}), 9.63 (dd, 2H, $J = 8.2$ Hz/1.3 Hz, H^1 and H^8); MS (ESI): $m/z = 393.1$ ($[M - 2PF_6^-]^{2+}$; calc.: 393.9).

4.1.3. *[Ru(bpy)$_2$(adppz)](PF$_6$)$_2$ (**1c**)*

79%, ^{1}H NMR (CD_3CN, 500.1 MHz): δ (ppm) = 6.35 (s, 2H, –NH_2), 7.33 (d, 1H, $J = 2.2$ Hz, H^{10}), 7.36–7.39 (m, 2H, $H^{pyridyl}$), 7.41–7.44 (m, 2H, $H^{pyridyl}$), 7.72 (dd, 1H, $J = 9.2$ Hz/2.2 Hz, H^{12}), 8.01 (dd, 2H, $J = 8.1$ Hz/4.4 Hz, H^2 and H^7), 8.09 (m, 4H, $H^{pyridyl}$), 8.14–8.19 (m, 5H, H^{13} and $H^{pyridyl}$), 8.25–8.29 (m, 2H, $H^{pyridyl}$), 8.45 (dd, 2H, $J = 4.4$ Hz/1.2 Hz, H^3 and H^6), 8.83–8.88 (m, 4H, $H^{pyridyl}$), 9.61 (dd, 2H, $J = 8.1$ Hz/1.2 Hz, H^1 and H^8); MS (ESI): $m/z = 355.6$ ($[M - 2PF_6^-]^{2+}$; calc.: 356.4).

4.1.4. *[Ru(bpy)$_2$(dadppz)](PF$_6$)$_2$ (**1d**)*

83%, ^{1}H NMR (CD_3CN, 500.1 MHz): δ (ppm) = 6.80 (s, 2H, H^{10} and H^{13}), 7.42 (t, 2H, $J = 6.9$ Hz/5.7 Hz, $H^{pyridyl}$), 7.64 (t, 2H, $J = 6.9$ Hz/5.7 Hz, $H^{pyridyl}$), 7.93 (dd, 2H, $J = 8.2$ Hz/5.7 Hz, $H^{pyriddyl}$), 8.03 (d, 2H, $J = 5.7$ Hz, $H^{pyridyl}$), 8.15 (m, 2H, $J = 8.2$ Hz/6.9 Hz/1.3 Hz, $H^{pyridyl}$), 8.18 (d, 2H, $J = 5.0$ Hz, H^2 and H^7), 8.26 (m, 2H, $J = 8.2$ Hz/6.9 Hz/1.3 Hz, $H^{pyridyl}$), 8.34 (d, 2H, $J = 4.4$ Hz, H^3 and H^6), 8.82 (d, 2H, $J = 8.2$ Hz, $H^{pyridyl}$), 8.86 (d, 2H, $J = 8.2$ Hz, $H^{pyridyl}$), 9.54 (d, 2H, $J = 7.5$ Hz, H^1 and H^8); MS (ESI): $m/z = 363.2$ ($[M - 2PF_6^-]^{2+}$; calc.: 363.9).

4.1.5. *[Ru(bpy)$_2$(dbrdppz)](PF$_6$)$_2$ (**1e**)*

54%, MS (ESI) m/z: 441.1 ($[M - 2PF_6^-]^{2+}$; ber.: 441.8), 361.2 ($[M - 2PF_6^- - 2Br]^{2+}$; calc.: 361.9).

4.2. General procedure for the synthesis of rhenium complexes

0.2 mmol (72 mg) $Re(CO)_5Cl$ and 0.2 mmol of the appropriate dppz ligand were solved in 25 ml of degassed toluene and refluxed for 24 h under Argon atmosphere. After a short time the complexes started to precipitate from the solution. After the reaction was completed the precipitate was filtered off while hot in order to avoid precipitation of unreacted dppz ligand. The crude product was washed and dried in vacuo.

4.2.1. *[Re(CO)$_3$(ndppz)Cl] (**2a**)*

86%, IR (KBr): $\tilde{\nu} = 2031$, 1905 cm^{-1}; ^{1}H NMR (DMSO-d_6, 500.1 MHz): δ (ppm) = 8.35 (dd, 1H, $J = 8.2$ Hz/4.9 Hz, H^7), 8.39 (dd, 1H, $J = 8.2$ Hz/4.9 Hz, H^2), 8.76 (dd, 1H, $J = 9.1$ Hz/2.2 Hz, H^{12}), 8.83 (d, 1H, $J = 9.1$ Hz, H^{13}), 9.34 (d, 1H, $J = 2.2$ Hz, H^{10}), 9.65 (dd, 1H, $J = 4.9$ Hz/1.3 Hz, H^6), 9.67 (m, 2H, H^1 and H^6), 9.92 (dd, 1H, $J = 8.2$ Hz/1.3 Hz , H^8).

4.2.2. *[Re(CO)$_3$(dndppz)Cl] (**2b**)*

75%, IR (KBr): $\tilde{\nu} = 2028$, 1918, 1891 cm^{-1}; ^{1}H NMR (DMSO-d_6, 500.1 MHz): δ (ppm) = 8.39 (dd, 2H, $J = 8.1$ Hz/4.8 Hz, H^2 and H^7), 9.08 (s, 2H, H^{10} and H^{13}), 9.67 (dd, 2H, $J = 4.8$ Hz/1.4 Hz, H^3 and H^6), 9.87 (dd, 2H, $J = 8.1$ Hz/1.4 Hz, H^1 and H^8).

4.2.3. *[Re(CO)$_3$(adppz)Cl] (**2c**)*

53%, IR (KBr): $\tilde{\nu} = 2021$, 1914, 1901 cm^{-1}; ^{1}H NMR (DMSO-d_6, 500.1 MHz): δ (ppm) = 7.26 (d, 1H, $J = 2.3$ Hz, H^{10}), 7.67 (dd, 1H, $J = 9.2$ Hz/2.3 Hz, H^{12}), 8.21 (dd, 1H, $J = 8.1$ Hz/4.4 Hz, H^2), 8.28 (dd, 1H, $J = 8.1$ Hz/4.4 Hz, H^7), 8.34 (d, 1H, $J = 9.2$ Hz, H^{13}), 9.50 (dd, 1H, $J = 4.4$ Hz/1.3 Hz, H^6), 9.57 (dd, 1H, $J = 4.4$ Hz/1.3 Hz, H^3), 9.74 (dd, 1H, $J = 8.1$ Hz/1.3 Hz, H^1), 9.89 (dd, 1H, $J = 8.1$ Hz/1.3 Hz, H^8).

4.2.4. *[Re(CO)$_3$(dadppz)Cl] (**2d**)*

61%, IR (KBr): $\tilde{\nu} = 2024$, 1901 cm^{-1}; ^{1}H NMR (DMSO-d_6, 500.1 MHz): δ (ppm) = 7.15 (s, 2H, H^{10} and H^{13}), 7.84 (dd, 2H, $J = 8.1$ Hz/4.9 Hz, H^2 and H^7), 9.39 (dd, 2H, $J = 4.9$ Hz/1.3 Hz, H^3 and H^6), 9.44 (dd, 2H, $J = 8.1$ Hz/1.3 Hz, H^1 and H^8).

4.2.5. *[Re(CO)$_3$(dbrdppz)Cl] (**2e**)*

63%, IR (KBr): $\tilde{\nu} = 2021$, 1913, 1897 cm^{-1}; ^{1}H NMR (DMSO-d_6, 500.1 MHz): δ (ppm) = 4.89 (s, 4H, -CH_2Br), 7.94 (dd, $J = 8.2$ Hz/4.5 Hz, 2H, H^2 and H^7), 8.39 (s, 2H, H^{10} and H^{13}), 9.44 (dd, 2H, $J = 4.5$ Hz/1.2 Hz, H^3 and H^6), 9.79 (dd, 2H, $J = 8.2$ Hz/1.2 Hz, H^1 and H^8).

4.3. General procedure for the synthesis of copper complexes

0.2 mmol (152 mg) of the complex $[Cu(CH_3CN)_2(PPh_3)_2](BF_4)$ and 0.2 mmol of the appropriate dppz ligand were solved in degassed dichloromethane and stirred at room temperature for 30 min under Argon atmosphere. The colour of the solution turned rapidly red indicating the formation of the copper dppz complexes. After completion of the reaction the solvent was evaporated under reduced pressure. The crude product was then dissolved in the minimum amount of dichloromethane. Slow addition of diethyl ether to this solution induced precipitation of the complexes. The complexes were dried in vacuo.

4.3.1. *[Cu(CH$_3$CN)$_2$(ndppz)](BF$_4$) (**3a**)*

77%; ^{1}H NMR (CD_2Cl_2, 500.1 MHz): δ (ppm) = 7.16–7.22 (m, 24H, $H^{2'}$, $H^{3'}$, $H^{5'}$ and $H^{6'}$), 7.35 (t, 6H, $J = 7.5$ Hz, $H^{4'}$), 8.05 (dd, 1H, $J = 8.2$ Hz/4.6 Hz, H^7), 8.64 (d, 1H, $J = 9.4$ Hz, H^{13}), 8.74 (dd, 1H, $J = 9.4$ Hz/2.5 Hz, H^{12}), 8.93 (dd, 1H, $J = 4.6$ Hz/1.8 Hz, H^3 and H^6), 9.38 (d, 1H, $J = 2.5$ Hz, H^{10}), 9.79 (dd, 1H, $J = 8.2$ Hz/1.8 Hz, H^1 and H^8); MS (ESI): $m/z = 914.7$ ($[M - BF_4^-]^+$; calc.: 915.4), 587.2 ($[Cu(PPh_3)_2]^+$, calc.: 588.1), 327.

4.3.2. *[Cu(CH$_3$CN)$_2$(dndppz)](BF$_4$) (**3b**)*

91%; ^{1}H NMR (CD_2Cl_2, 500.1 MHz): δ (ppm) = 7.16–7.22 (m, 24H, $H^{2'}$, $H^{3'}$, $H^{5'}$ and $H^{6'}$), 7.35 (t, 6H, $J = 7.5$ Hz, $H^{4'}$), 7.99 (dd, 2H, $J = 8.2$ Hz/5.0 Hz, H^2 and H^7), 8.86 (d, 2H, $J = 5.0$ Hz, H^3 and H^6), 9.07 (s, 2H,

H^{10} and H^{13}), 9.74 (dd, 2H, $J = 8.2$ Hz/1.3 Hz, H^1 and H^8); MS (ESI): $m/z = 959.8$ ($[M - BF_4^-]^+$; calc.: 960.4), 587.2 ($[Cu(PPh_3)_2]^+$, calc.: 588.1), 372.

*4.3.3. [Cu(CH$_3$CN)$_2$(adppz)](BF$_4$) (**3c**)*

88%; ^{1}H NMR (CD_2Cl_2, 500.1 MHz): δ (ppm) = 7.16–7.22 (m, 24H, $H^{2'}$, $H^{3'}$, $H^{5'}$ and $H^{6'}$), 7.35 (t, 6H, $J = 7.5$ Hz, $H^{4'}$), 7.39 (d, 1H, $J = 9.1$ Hz, H^{10}), 7.81 (dd, 1H, $J = 9.1$ Hz/2.2 Hz, H^{12}), 8.18 (dd, 1H, $J = 8.0$ Hz/4.3 Hz, H^2 and H^7), 8.24 (d, 1H, $J = 2.2$ Hz, H^{13}), 8.84 (dd, 1H, $J = 4.3$ Hz/1.4 Hz, H^3 and H^6), 9.68 (dd, 1H, $J = 8.0$ Hz/1.3 Hz, H^1 and H^8); MS (ESI): $m/z = 884.8$ ($[M - BF_4^-]^+$; calc.: 885.5), 587.2 ($[Cu(PPh_3)_2]^+$, calc.: 588.1), 297.

*4.3.4. [Cu(CH$_3$CN)$_2$(dadppz)](BF$_4$) (**3d**)*

85%; ^{1}H NMR (CD_2Cl_2, 500.1 MHz): δ (ppm) = 6.27 (s, 4H, N*H*$_2$), 7.16–7.22 (m, 26H, H^{10}, H^{13}, $H^{2'}$, $H^{3'}$, $H^{5'}$ and $H^{6'}$),7.35 (t, 6H, $J = 7.5$ Hz, $H^{4'}$), 8.06 (dd, $J = 8.1$ Hz/4.5 Hz, 2H, H^2 and H^7), 8.67 (dd, $J = 4.5$ Hz/1.8 Hz, 2H, H^3 and H^6), 9.59 (dd, $J = 8.1$ Hz/1.8 Hz, 2H, H^1 and H^8); MS (ESI): $m/z = 899.7$ ($[M - BF_4^-]^+$; calc.: 900.5), 587.2 ($[Cu(PPh_3)_2]^+$, calc.: 588.1), 312.

*4.3.5. [Cu(CH$_3$CN)$_2$(dbrdppz)](BF$_4$) (**3e**)*

67%; ^{1}H NMR (CD_2Cl_2, 500.1 MHz): δ (ppm) = 4.88 (s, 4H, –C*H*$_2$Br), 7.16–7.22 (m, 24H, $H^{2'}$, $H^{3'}$, $H^{5'}$ and $H^{6'}$), 7.35 (t, 6H, $J = 7.5$ Hz, $H^{4'}$), 7.97 (dd, 2H, $J = 8.2$ Hz/5.0 Hz, H^2 and H^7), 8.15 (s, 2H, H^{10} and H^{13}), 8.82 (dd, 2H, $J = 5.0$ Hz/1.3 Hz, H^3 and H^6), 9.69 (dd, 2H, $J = 8.2$ Hz/1.3 Hz, H^1 and H^8); MS (ESI): $m/z = 895.3$ ($[M - BF_4^- - 2Br]^+$; calc.: 896.5), 587.2 ($[Cu(PPh_3)_2]^+$, calc.: 588.1), 308.

*4.4. General procedure for the synthesis of amino-functionalized Ru(II) complex **1c** and Cu(I) complex **3c** by reduction of the nitro-functionalized complexes*

150 mg of the nitro-substituted complexes **1a** or **3a** and 30 mg Pd/C (10%) were suspended in ethanol. The resulting mixture was reduced at room temperature for 24 h under a hydrogen atmosphere (5 bar) in a Parr apparatus. After completion of the reaction the catalyst was filtered off and the residue washed with boiling ethanol. The solvent was evaporated under reduced pressure. The solid obtained was dried in vacuo. The amino-functionalized complexes $[Ru(bpy)_2(adppz)](PF_6)_2$ and $[Cu(PPh_3)_2(adppz)](BF_4)$ were obtained in 91% and 89%, respectively. For analytical data, see above.

*4.5. General procedure for the synthesis of diamino-functionalized Ru(II) complex **1d** ans Cu(I) complex **3d** by reduction of the dinitro-functionalized complexes*

150 mg of the nitro-substituted $[Cu(CH_3CN)_2L]^{2+}$ (L = ndppz, dndppz) and 30 mg Pd/C (10%) were suspended in ethanol. The resulting mixture was reduced at room temperature for 24 h under a hydrogen atmosphere (5 bar) in a Parr apparatus. After completion of the reaction the catalyst was filtered off and the residue washed with boiling ethanol. The solvent was evaporated under reduced pressure. The solid obtained was dried in vacuo. The amino-functionalized complexes $[Ru(bpy)_2(dadppz)](PF_6)_2$ and $[Cu(CH_3CN)_2(dadppz)](BF_4)$ were both obtained in 91% yield, respectively. For analytical data, see above.

Acknowledgement

Financial support of the Fonds der Chemischen Industrie and the Innovationsfonds der Universität Bielefeld is gratefully acknowledged.

References

[1] (a) C.M. Dupureur, J.K. Barton, Inorg. Chem. 36 (1997) 33;
(b) T.K. Schoch, J.L. Hubbard, C.R. Zoch, G.-B. Yi, M. Soerlie, Inorg. Chem. 35 (1996) 4383;
(c) R.E. Holmlin, J.K. Barton, Inorg. Chem. 34 (1995) 7;
(d) Y. Jenkins, A.E. Friedman, N.J. Turro, J.K. Barton, Biochemistry 31 (1992) 10809;
(e) V.W.-W. Yam, K.K.-W. Lo, K.-K. Cheung, R.Y.-C. Kong, J. Chem. Soc., Dalton Trans. (1997) 2067.
[2] (a) J.-C. Chambron, J.-P. Sauvage, Chem. Phys. Lett. 182 (1991) 603;
(b) A.E. Friedman, J.-C. Chambron, J.-C. Sauvage, N.J. Turro, J.K. Barton, J. Am. Chem. Soc. 112 (1990) 4960.
[3] M. Graetzel, Coord. Chem. Rev. 111 (1991) 167.
[4] M.K. Nazeeruddin, A. Kay, I. Ridicio, R. Humphrey-Baker, E. Mueller, P. Liska, N. Vlachopoulos, M. Graetzel, J. Am. Chem. Soc. 115 (1993) 6382.
[5] (a) J.-C. Chambron, J.-P. Sauvage, Nouv. J. Chim. 9 (1985) 527;
(b) E. Amouyal, A. Homsi, J.-C. Chambron, J.-P. Sauvage, J. Chem. Soc., Dalton Trans. (1990) 1841.
[6] V. Balzani, A. Juris, Coord. Chem. Rev. 211 (2001) 97.
[7] N. Armaroli, Chem. Soc. Rev. 30 (2001) 113.
[8] V.W.-W. Yam, Chem. Commun. (2001) 789.
[9] L. De Cola, P. Belser, Coord. Chem. Rev. 177 (1998) 301.
[10] (a) D.M. Guldi, M. Maggini, E. Menna, G. Scorrano, P. Ceroni, M. Marcaccio, F. Paolucci, S. Roffia, Chem. Eur. J. 7 (2001) 1597;
(b) A. Polese, S. Mondini, A. Bianco, C. Toniolo, G. Scorrano, D.M. Guldi, M. Maggini, J. Am. Chem. Soc. 121 (1999) 3446;
(c) D. Armspach, E.C. Constable, F. Diederich, C.E. Housecroft, J.F. Nierengarten, Chem. Eur. J. 4 (1998) 723;
(d) M. Maggini, D.M. Guldi, S. Mondini, G. Scorrano, F. Paolucci, P. Ceroni, S. Roffia, Chem. Eur. J. 4 (1998) 1992;
(e) N.S. Sacriciftci, F. Wudl, A.J. Heeger, M. Maggini, G. Scorrano, M. Prato, J. Bourassa, P.C. Ford, Chem. Phys. Lett. 247 (1995) 510.
[11] (a) N. Armaroli, C. Boudon, D. Felder, J.P. Gisselbrecht, M. Gross, G. Marconi, J.F. Nicoud, J.F. Nierengarten, V. Vicinelli, Angew. Chem. Int. Ed. 38 (1999) 3730;
(b) N. Armaroli, F. Diederich, C.O. Dietrich-Buchecker, L. Flamigni, G. Marconi, J.F. Nierengarten, J.-P. Sauvage, Chem. Eur. J. 4 (1998) 406.
[12] N. Armaroli, G. Accorsi, D. Felder, J.F. Nierengarten, Chem. Eur. J. 8 (2002) 2314.
[13] A. Kleineweischede, J. Mattay, Eur. J. Org. Chem., (2006) 947.
[14] D.R. McMillin, R.E. Gamache Jr., J.R. Kirchhoff, A.A. Del Paggio, in: K.D. Karlin, J. Zubieta (Eds.), Copper Coordination Chemistry: Biochemical and Inorganic Perspectives, Academic Press, New York, 1983, p. 233.

[15] J.V. Caspar, T.J. Meyer, J. Phys. Chem. 87 (1983) 952.
[16] B.P. Sullivan, D.J. Salmon, T.J. Meyer, Inorg. Chem. 17 (1978) 3334.
[17] P. Lincoln, A. Broo, B. Norden, J. Am. Chem. Soc. 118 (1996) 2644.
[18] (a) C.-S. Choi, L. Mishra, T. Mutai, K. Araki, Bull. Chem. Soc. Jpn. 73 (2000) 2051;
T. Akasaka, H. Inoue, M. Kuwabara, T. Mutai, J. Otsuki, K. Araki, Dalton Trans. (2003) 815.
[19] (a) J.-C. Chambron, J.-P. Sauvage, E. Amouyal, P. Koffi, Nouv. J. Chim. 9 (1985) 527;
(b) L.E. Orgel, J. Chem. Soc. (1961) 3683.
[20] A. Arancabia, J. Concepcion, N. Daire, G. Leiva, A.M. Leiva, B. Loeb, R. del Rio, R. Diaz, A. Francois, M. Saldivia, J. Coord. Chem. 54 (2001) 323.
[21] V.M.S. Gil, J.N. Murrell, Trans. Faraday Soc. 60 (1964) 248.
[22] R.W. Balk, D.J. Stufkens, A. Oskam, J. Chem. Soc., Dalton Trans. (1981) 1124.
[23] L. Worl, R. Duesing, P. Chen, L.D. Ciana, T.J. Meyer, J. Chem. Soc., Dalton Trans. (1991) 849.
[24] M.R. Waterland, K.C. Gordon, J.J. McGarvey, P.M. Jayaweera, J. Chem. Soc., Dalton Trans. (1998) 609.
[25] P.F. Barron, J.C. Dyason, L.M. Engelhardt, P.C. Healy, A.H. White, Aust. J. Chem. 38 (1985) 261.
[26] A. Lange, P. Tavan, D. Schröder, H. Baumgärtel, Ber. Bunsenges. Phys. Chem. 85 (1981) 78.
[27] V. Balzani, A. Juris, Coord. Chem. Rev. 211 (2001) 97–115.
[28] (a) M.N. Ackermann, L.V. Interrante, Inorg. Chem. 23 (1984) 3904;
(b) J.C. Chambron, J.P. Sauvage, E. Amouyal, P. Koffi, J. Chem. Soc., Dalton Trans. (1990) 1841;
(c) J. Fees, W. Kaim, M. Moscherosch, W. Matheis, J. Klima, M. Krejcik, S. Zalis, Inorg. Chem. 32 (1993) 166.
[29] A. Klein, C. Vogler, W. Kaim, Organometallics 15 (1996) 236.
[30] C. Vogler, W. Kaim, Z. Naturforsch. Teil B 47 (1992) 1057.
[31] W. Kaim, H.E.A. Kramer, C. Vogler, J. Rieker, J. Organomet. Chem. 367 (1989) 107.
[32] M.R. Waterland, T.J. Simpson, K.C. Gordon, A.K. Burrell, J. Chem. Soc., Dalton Trans. (1998) 165.
[33] M.R. Waterland, K.C. Gordon, J. Raman Spectrosc. 31 (2000) 243.
[34] (a) S.E. Page, K.C. Gordon, A.K. Burrell, Inorg. Chem. 37 (1998) 4452;
(b) S.M. Scott, K.C. Gordon, A.K. Burrell, Inorg. Chem. 35 (1996) 2452.